Numerical Simulations of Fully Nonlinear Wave Motions in a Digital Wave Tank

JONG-CHUN PARK*, KYUNG-SUNG KIM*
*Department of Naval Architecture and Ocean Engineering
Pusan National University
30 Jangjeon-dong, Geumjeong-gu, Pusan, Korea

Abstract: A digital wave tank (DWT) simulation technique has been developed by authors to investigate the interactions of fully nonlinear waves with 3D marine structures. A finite-difference/volume method and a modified marker-and-cell (MAC) algorithm have been used, which are based on the Navier-Stokes (NS) and continuity equations. The fully nonlinear kinematic free-surface condition is implemented by the marker-density function (MDF) technique or the Level-Set (LS) technique developed for one or two fluid layers.
In this paper, some applications for various engineering problems with free-surface are introduced and discussed. It includes numerical simulation of marine environments by simulation equipments, fully nonlinear wave motions around offshore structures, nonlinear ship waves, ship motions in waves and marine flow simulation with free-surface.
From the presented simulations, it seems that the developed DWT simulation technique can handle various engineering problems with free-surface and reliably predict hydrodynamic features due to the fully-nonlinear wave motions interacting with such marine structures.

Key-Words: Digital wave tank (DWT), Nonlinear wave motions, Navier-Stokes (N-S) equation, Ship motion simulation, Numerical wavemaker, Wave-structure interaction

1 Introduction

Virtual reality by use of computational fluid dynamics (CFD) has been realized by high accuracy of simulation technique and high performance of computer power. Especially, System-Design-By-Simulation techniques for marine structures are quite effective for design of the structures, based on understanding of physical phenomena. Of these, a digital wave tank (DWT) simulation techniques have been also developed to more advanced technology, and it can be first utilized for the purpose of elucidating nonlinear physical phenomena related to nonlinear wave motions, and then applied to the purpose of designing or inventing new systems in ocean or coasts. In near future, as shown in Fig.1, it is believed that all experimental towing tank tests would be alternated with digital towing tank tests, including not only resistance tests but also motion and maneuvering tests in random sea conditions.

However, the numerical implementation of the fully nonlinear free-surface condition is in general complicated and difficult. The major difficulties associated with the fully nonlinear free-surface simulations around 3D structures consist in (i) the complicated nonlinear free-surface boundary conditions that have to be satisfied on the instantaneous free-surface position not known a priori, (ii) various types of numerical instabilities, (iii) the appropriate open-boundary conditions representing open-sea condition, (iv) the treatment of body-surface condition of complex geometry in the vicinity of free-surface, and (v) large CPU time and storage required to keep satisfactory degree of accuracy.

In the present study, efforts have been focused on the nonlinear free-surface motions using a marker-density function (MDF) method. The method is basically similar to the volume-of-fluid (VOF) method (Hirt and Nichols, 1981) in that the interface can be defined by the volume fraction of fluid within a cell. However, the numerical treatment of the MDF method is more easily applicable to complicated free-surface flows around a 3D body. The MDF technique was originally devised by Miyata et al. (1988) to cope with two-layer flows involving strongly interacting interface. However, the accuracy of the method in the wave formation was not fully verified at that time. Park et al. (1993) improved the accuracy of the interface treatment through numerical experiments with non-breaking regular periodic waves. The technique has since been upgraded and used for various engineering problems including the 2D breaking waves (Park & Miyata, 1994), 3D breaking waves around a ship and an offshore structure (Miyata & Park, 1995; Miyata et al., 1996; Sato et al, 1999; Orihara & Miyata, 2000), the fully-nonlinear DWT simulations (Park et al., 1999 & 2003; Kim et al., 2000), the bubbly flow (Kanai & Miyata, 2001), etc. Similar methods using the same MDF concept have been developed recently, which include the continuum surface force (CSF) method by Brackbill et al. (1992), the CIP method by Yabe et al. (1993), and the level-set method by Sussman et al. (1994).

In the present study, emphasis is put on a DWT simulation technique and their applications. The numerical simulation method for the DWT is briefly introduced in Sec.2. The capability of the simulation equipments of marine environments are demonstrated in Sec.3. In Sec.4, various applications for the engineering problems with

fully-nonlinear wave motions are introduced. Some concluding remarks are given in Sec.5.

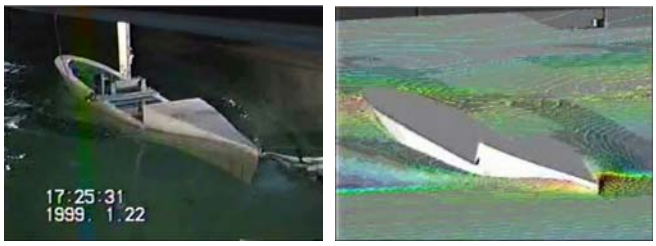

Fig.1. Ship model tests in an experimental tank (left) and a DWT (right).

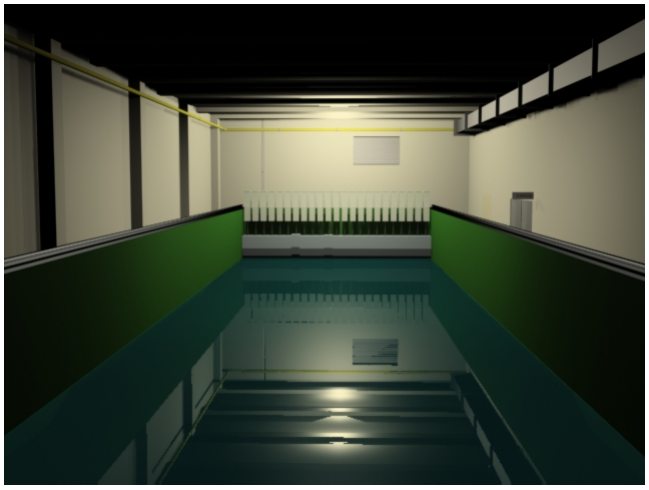

Fig.2. Schematic view of DWT.

- Finite-Difference/Volume Method
- Modified-**MAC** algorithm
- **H-H** *or* **O-H Grid System**
- **SOR** iteration method for solving pressure field
- **MDF** *or* **LS** technique for nonlinear free-surface movement
- **Large-Eddy-Simulation** *or* **RANS** for turbulent flow *with wall function*
- 3rd-order **TVD scheme** *with limiter* for Advection Term
- 2nd-order **Adams-Bashforth** scheme for time integration

Fig.3. Outline of the developed DWT Simulation Technique.

2. Numerical Implementation of DWT

2.1 DWT simulation techniques

Fig.2 shows a schematic view of a DWT, and the outline of the developed DWT simulation technique is summarized in Fig.3. The governing equations, Navier-Stokes (N-S) and continuity equations, are solved in the computational domain and the boundary values updated at each time step by a finite-difference/ volume time-marching scheme in the framework of rectangular/curvilinear coordinate system. The nonlinear free-surface configuration is mainly determined by the MDF technique. For the turbulence model, SGS model is employed. And for the convective terms a flux-split method similar to a third-order TVD scheme with limiter is used. The second-order Adams-Bashforth method is used for the time-differencing. A second-order central differencing scheme is employed for the diffusive terms.

The solution algorithm can be referred from Park et al.(1999 & 2003), Miyata & Park(1995), Sato et al.(1999).

2.2 Nonlinear Free Surface Conditions

The configuration of the interface is determined by applying the fully-nonlinear free-surface condition. At the free surface, the following fully nonlinear kinematic and dynamic conditions can be applied neglecting the viscous stress and surface tension:

$$\frac{\partial M_\rho}{\partial t} + \mathbf{u} \cdot \nabla M_\rho = 0 . \qquad (1)$$

$$p = 0 \qquad (2)$$

where, the MDF M_ρ takes the value between 0 and 1 all over the computational domain. Eq. (1) is calculated at each time step and the free-surface location is determined to be a point where the MDF takes the mean value as

$$\overline{M}_\rho = \frac{1}{2}. \qquad (3)$$

In the present study, in order to prevent from the excessive diffusion numerically in the vicinity of interface, we do not solve directly Eq. (1) but solve Eq. (4) introducing both the *mapping function* and the *re-distribution algorithm* (Sussman et al., 1994) to the previous MDF technique (Miyata and Park, 1995). As a mapping function, the distance function, ϕ, is employed in Eq. (1) and defined continuously in the whole domain of simulation.

$$\frac{\partial \phi}{\partial t} + u\frac{\partial \phi}{\partial x} + v\frac{\partial \phi}{\partial y} + w\frac{\partial \phi}{\partial z} = 0 . \qquad (4)$$

Then, the distribution of MDF at each time step is updated maintaining the interface location as,

$$M_\rho = \begin{cases} M_\rho^1 & \text{if } \phi > \varepsilon_0 \\ M_\rho^2 & \text{if } \phi < -\varepsilon_0 \\ \overline{M}_\rho + \tilde{M}_\rho \cdot (\phi/\varepsilon_0) & \text{otherwise} \end{cases} \qquad (5)$$

where, $\tilde{M}_\rho = \left(M_\rho^1 - M_\rho^2\right)/2$ and $\varepsilon_0 = 2(\Delta x)_{\min}$.

The transport equation (4) of ϕ can be solved using the high-order accurate scheme, i.e. the fourth-order Runge-Kutta scheme for time differencing and the 3rd-order MUSCL scheme for convection term.

On the other hand, the dynamic free-surface condition

of Eq. (2) is implemented by the so-called "irregular star" technique (Chan and Street, 1970) in the solution process of the Poisson equation for the pressure. In the free-surface problems, it is very important to extrapolate the pysical values onto the free-surface, so the pressure on it is determined by extrapolating from the neighboring fluid to the free-surface location. The pressures are extrapolated with zero gradient in the approximately normal direction to the free surface while the static pressure difference in the vertical direction due to the gravity is taken into consideration. Similarly, the velocities are extrapolated at the interface with approximately no normal gradient from fluid region. This treatment grossly accords with the viscous tangential condition at the free surface.

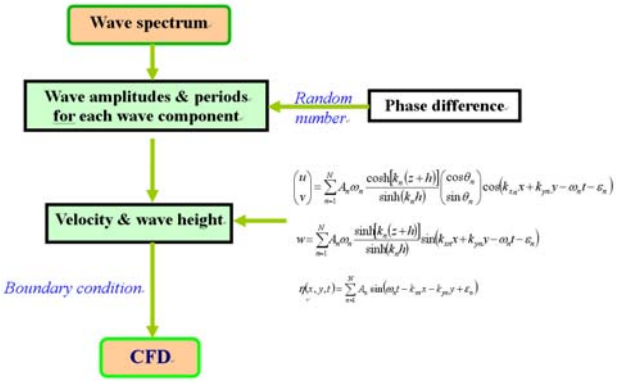

Fig.4. Procedure of imposing boundary condition on wave panel.

2.3 Other Boundary Conditions

At the inflow boundary, i.e., the simulation equipments of marine environments, i.e. a numerical wavemaker, is established by prescribing the inflow velocities based on the water particle velocities of the linear wave (or Stokes second-order wave), which is like a flexible flap wavemaker. For multi-directional wave generation, a snake-like wavemaker motion is used on the basis of linear wavemaker theory (Dean and Darlymple, 1991). Fig.4 indicates a procedure of imposing boundary condition on wave panels.

For the sidewall boundary, the diverse boundary conditions can be imposed flexibly. For instances, the free-slip rigid wall and the weakly-opened boundary conditions were tested in Kim et al. (2001), and one side of a dual-face-snake-type wavemaker with the other side of a numerical beach was employed to increase the effective test area in Kim et al. (2000).

One of the most critical issues for fully-nonlinear digital wave tank simulations is the numerical implementation of a robust downstream open boundary condition. A well-designed open boundary condition is particularly important to reduce the size of the computational domain. In the present study, an artificial damping scheme (Park et al., 1999) is employed in the added dissipation zone to dissipate all the wave energy of outgoing waves, and the mesh size is gradually increased in the horizontal direction to provide additional numerical damping.

At the bottom boundary of the DWT, zero-normal-gradient boundary conditions are given for the velocity and the hydrostatic pressure is given assuming that the vertical distances from the interface are sufficiently large in comparison with the wave height of interest.

No-slip body boundary condition is imposed on the body surface. A special treatment of the free-surface location at the intersection with the body surface has been made so that the possible singularity is removed, i.e. the values of MDF on the body surface are extrapolated with zero-normal gradient from the fluid region.

3. Simulation Equipments of Marine Environments

3.1 Numerical Simulation of Irregular Wave

Numerical simulation of irregular wave was made by superposing 64 wave components selected from the Bretschneider-Mitsuyasu-type wave energy spectrum modified by Goda (1987) for coastal zone, which is expressed as:

$$S(f) = 0.205 H_{1/3}{}^2 T_{1/3}{}^{-4} f^5 \exp\left[-0.75\left(T_{1/3} f\right)\right]^{-4} \quad (6)$$

where, f is the frequency, $H_{1/3}$ significant wave height, and $T_{1/3}$ significant wave period. The wave amplitude of each component is calculated by $A = \sqrt{2S(f)df}$, where df is an interval of frequency between neighboring components. In this study, the significant wave height and period are set at $H_{1/3}$ =0.05m and $T_{1/3}$ =1.33s, respectively.

Two cases of numerical simulation are tested with coarser (CASE 1) and finer (CASE 2) grid conditions, and the condition is detailed in Table 1.

Table.1. Condition of calculation for 2D irregular wave.

	CASE 1	CASE 2
Δx	$L_{1/3}$/50	$L_{1/3}$/150
Δz	$H_{1/3}$/20	$H_{1/3}$/20
Δt	$T_{1/3}$/800	$T_{1/3}$/2000

In Fig.5, the simulated wave spectra are quantitatively compared with the target spectrum. The spectral analysis is performed by FFT algorithm, which averaged through 5 times analyses with different phase angles. For CASE 2, overall agreement is excellent except for high frequency region ($f >> 1.5Hz$) where the numerical dissipation of energy is remarkable.

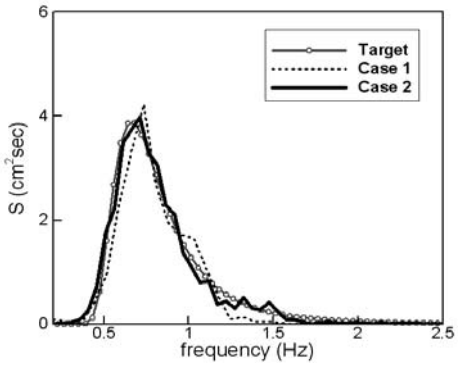

Fig.5. Comparison of target and simulated wave spectra for 2D irregular wave.

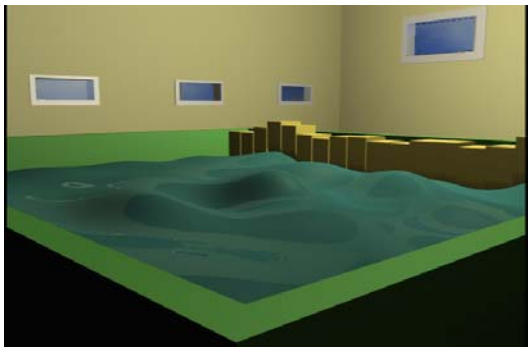

Fig.6(a). Snapshot of bull's-eye wave field in a DWT.

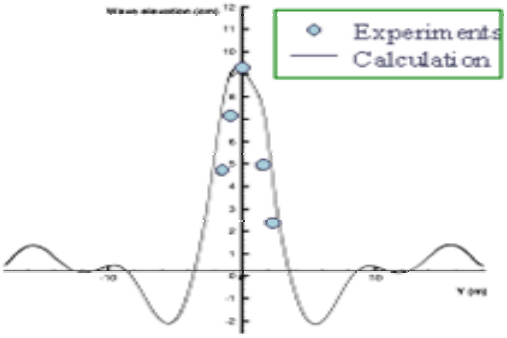

Fig.6(b). Wave profile of cross section along the focal point.

3.2 Numerical Generation of Bull's-eye Waves

The bull's-eye waves can be generated by phase control of wavemaker panels, which is based on the fact that a group of waves is propagated towards a common focusing point. The phase difference at two different segments can be determined from $\boldsymbol{\varepsilon} = \mathbf{k}\left(\mathbf{r}_2 - \mathbf{r}_1\right)$, where $\mathbf{k}$ is the wave number and $\mathbf{r}$ is the distance from the respective segment to the common focusing point. The bull's-eye waves were designed to converge toward a focal point along the centerline. The wave height and period are 20mm and 1.44s, respectively. Fig.6(a) shows a snapshot of the bull's-eye wave simulation. It is seen that the current method can generate the directional wave field as designed. Fig.6(b) shows the cross section of wave profile along the focus, in which the circle presents the experimental result conducted in the OTRC wave basin at Texas A&M University. We can see that most wave energy propagates toward the focal point, so wave amplitudes are very high there but small elsewhere. In this simulation, the maximum wave height probed at a focal point was 9-times higher than the incident wave amplitude.

Fig.7. A Wing-In-Ground (WIG) ship.

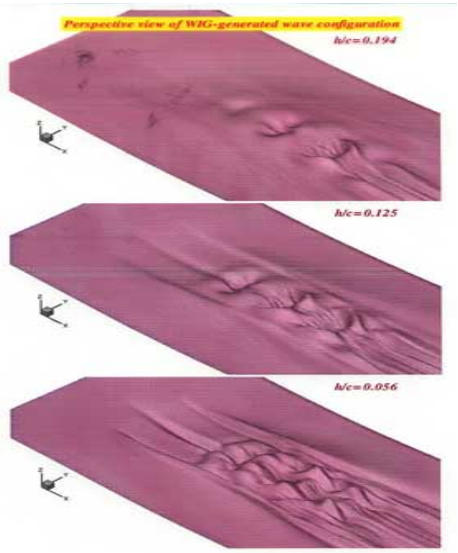

Fig.8. Waves generated by a WIG ship.

4. Some Applications of Fully Nonlinear Wave Motions

4.1 Waves Generated by High Speed Vessels

A numerical simulation is performed for the 3D flow around a Wing-In-Ground (WIG) effect ship with a complex geometry, as shown in Fig.7. The air and water flows are simultaneously simulated in the time-marching solution procedure. The numerical calculations around a WIG ship advancing in calm water are conducted and the flow characteristics for the nonlinear wave motions generated by a WIG ship can be discussed.

The perspective views of the WIG-generated waves are shown in Fig.8, in which wave heights are enlarged 5000

times vertically. As the altitude ratio decreases, waves are complicatedly developed and propagated to the downstream while the wave propagation in the lateral direction is restrained due to the existence of the side-endplate.

4.2 Ship Motions in Waves

A finite-volume method has been developed for the ship motion simulation in waves. The motion of the ship is treated in a fixed coordinate system, which means that the grid system also moves according to the ship's motion, as shown in Fig.9. The origin of the coordinate system is at the center of the ship, and the trajectory and attitude of the ship are determined in the space-fixed coordinates. The solution procedure for the Navier-Stokes equation is combined with that for the motion equations in six degree-of-freedom. The O-H type grid system surrounds the hull is employed and the motion of the structure is represented by external forces in the Navier-Stokes equation as shown in Fig.10.

Fig.11 shows the 3-D snapshots of the large amplitude of roll motion of a Series 60 model (Cb=0.6) advancing at Froude number 0.2 in oblique following waves of λ/L =2, H/L =0.012, oblique angle=20^o. In this simulation, 3-degree-of-freedom motion (Heave, Pitch and Roll motions are free). The very unstable ship motions with over the 20 degrees of rolling are observed caused by following and quartering waves. However, this simulation is not continued any longer due to the grid system problem using a moving coordinate.

To handle in convenient the ship motion with large amplitude, a composite grid system is employed, which an inner O-H grid system including the ship model is overlapped onto the DWT (outer grid system) as shown in Fig.12(left). By use of this grid system, the marine environments and ship motions are treated in two separated grid systems, which the marine environments for waves, tide, wind, etc. are generated in the outer grid system and the large motions of ship is treated by moving and rotating the whole of the inner grid system. However, the numerical technique for interface where two grid systems are overlapped is quite important and must be carefully treated conserving the mass and flux on it. In the present method, a linear interpolation technique was tested and used. Ultimate Goals of the present method are to simulate the extremely nonlinear ship motion, i.e. Slamming and Capsizing motions in large-amplitude waves. In Fig.12, Motion simulation using a composite grid system is examined for a Series 60 ship advancing at Fn=0.316 in still-water with 20 degrees of enforced roll motion.

5 Concluding Remarks

A DWT simulation technique based on the CFD has been developed in order to elucidate nonlinear physical phenomena and in order to design such marine systems with high performance.

In this paper, some applications for various engineering problems with free-surface were introduced and discussed. It included numerical simulation of marine environments by simulation equipments, fully nonlinear wave motions around offshore structures, nonlinear ship waves, ship motions in waves and marine flow simulation with free-surface.

In near future, the developed technology will be applied usefully to multipurpose research in marine environmental engineering fields.

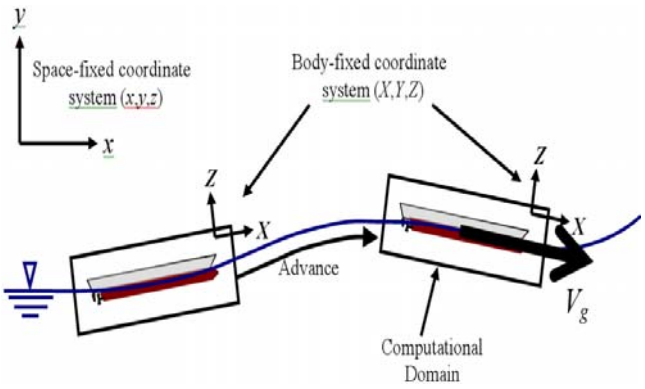

Fig.9. Governing Equations for motion simulation.

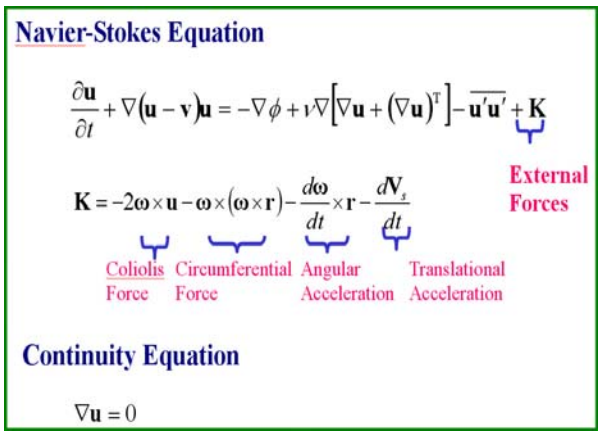

Fig.10. Governing Equations for motion simulation.

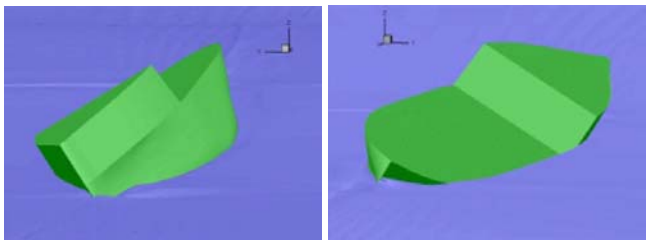

Fig.11. 3D snapshots of Series 60 model advancing in oblique following sea (left: front view, right: rear view).

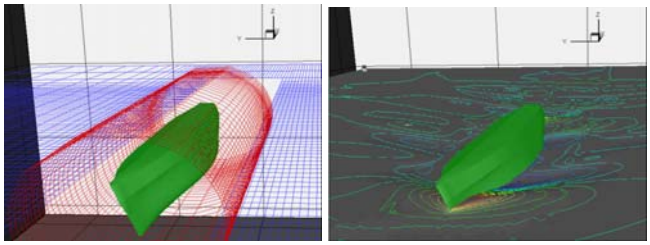

Fig.12. Motion simulation of a Series 60 ship advancing and rolling with large amplitude (left: composite grid system, right: wave contour).

References:

[1] Brackbill, J.U., Kothe, D.B. and Zemach, C. (1992), "A Continuum Method for Modeling Surface Tension", J. of Comp. Physics, 100, 335-354.

[2] Chan, R.K.C. and Street, R.L. (1970), "A Computer Study of Finite Amplitude Water Waves", J. of Comp. Physics, 6, 68-94.

[3] Dean, R.G. and Dalrymple, R.A. (1991), "Water Wave Mechanics for Engineers and Scientists", World Scientific Publ.

[4]Goda, Y. (1987), "Standard Spectra and Statistics of Sea Waves Derived by Numerical Simulation", 34th Japanese Conf. on Coastal Engineering, 131-135.

[5] Hirt, C.W. and Nichols, B.D. (1981), "Volume of Fluid (VOF) Method for the Dynamics of Free Boundaries ", J. of Comp. Physics, 39, 201-225.

[6] Kanai, A and Miyata, H. (2001), "Direct numerical simulation of wall turbulent flows with microbubbles", Int. J. for Numerical Methods in Fluids, 35, 593-615.

[7] Kim, M.H., Niedzwecki, J.M., Roesset, J.M., Park, J.C., Hong, S.Y. & Tavassoli, A. (2001), "Fully Nonlinear Multdirectional Waves by a 3-D Viscous Numerical Wave Tank", J. of Offshore Mechanics and Arctic Engineering, 123, 124-133.

[8] Kim, M.H., Park, J.C. and Tavassoli, A. (2000), "Fully Nonlinear Multi-directional Wave Simulations by 3D Numerical Wave Tanks", Proc. 14th Int. Conf. on Hydrodynamics, Yokohama.

[9] Miyata, H., Katsumata, M., Lee, Y.G. and Kajitani, H. (1988), "A Finite-Difference Simulation Method for Strongly Interacting Two-Layer Flow", J. of Marine Science and Technology, 163, 1-16.

[10] Miyata, H., Kanai, A. Kawamura, T. and Park, J.C. (1996), "Numerical simulation of three-dimensional breaking waves", J. of Marine Science and Technology, 1, 183-197.

[11] Miyata, H. and Park, J.C. (1995), "Ch.5 Wave Breaking Simulation", Advances in Fluid Mechanics, Potential Flow of Fluids, ed. M. Rahman, Computational Mechanics Publications, UK., 149-176.

[12] Orihara, H. and Miyata, H. (2000), "Numerical Simulation Method for Flows About a Semi-Planing Boat with a Transom Stern", J. of Ship Research, 44-3, 170-185.

[13] Park, J.C., Kim, M.H. and Miyata, H. (1999), "Fully Non-linear Free-Surface Simulations by a 3D Viscous Numerical Wave Tank", Int. J. for Numerical Methods in Fluids, 29, 685-703.

[14] Park, J.C., Kim, M.H. and Miyata, H. (2003), "Fully nonlinear numerical wave tank (NWT) simulations and wave run-up prediction around 3-D structures ", Ocean Engineering, 30, 1969-1996.

[15] Park, J.C. and Miyata, H. (1994), "Numerical Simulation of the Nonlinear Free-Surface Flow Caused by Breaking Waves", ASME FED-vol.181, Free-Surface Turbulence, 155-168, Lake Tahoe.

[16] Park, J.C., Zhu, M. and Miyata, H. (1993), "On the Accuracy of Numerical Wave Making Techniques", J. Soc. Naval Architecture of Japan, 173, 35-44.

[17] Sato, Y., Miyata, H. and Sato, T. (1999), "CFD Simulation of 3D Motion of a Ship in Waves", J. of Marine Science and Technology, 4, 108-116.

[18] Sussman, M., Smereka, P. and Osher, S. (1994), "A Level Set Approach for Computing Solutions to Incompressible Two-Phase Flow", J. of Comp. Physics, 114, 146-159.

[19] Yabe, T., Xiao, F. and Wang, P. (1993), "Description of Complex and Sharp Interface during Shock Wave Interaction with Liquid Drop", J. of Phys. Soc. Japan, 62, 2537-2540.